Journal of Applied Polymer Science

The Optical Properties of PVA/TiO_2 Composite Nanofibers

Parastoo Ahmadpoor,[1] Ali Shams Nateri,[1,2] Vahid Motaghitalab[1]
[1]Textile Engineering Department, University of Guilan, Rasht, Iran
[2]Center of excellence for color science and technology, Tehran, Iran
Correspondence to: A. S. Nateri (E-mail: a_shams@guilan.ac.ir)

ABSTRACT: The electrospun nanofibers emerge several advantages because of extremely high specific surface area and small pore size. This work studies the effect of PVA nanofibers diameter and nano-sized TiO_2 on optical properties as reflectivity of light and color of a nanostructure assembly consisting polyvinyl alcohol and titanium dioxide (PVA/TiO_2) composite nanofibers prepared by electrospinning technique. The PVA/TiO_2 composite spinning solution was prepared through incorporation of TiO_2 nanoparticles as inorganic optical filler in polyvinyl alcohol (PVA) solution as an organic substrate using the ultrasonication method. The morphological and optical properties of collected composites nanofibers were highlighted using scanning electron microscopy (SEM) and reflective spectrophotometer (RS). The reflectance spectra indicated the less reflectance and lightness of composite with higher nanofiber diameter. Also, the reflectance and lightness of nanofibers decreased with increasing nano-TiO_2 concentration. © 2013 Wiley Periodicals, Inc. J. Appl. Polym. Sci. 000: 000–000, 2013

KEYWORDS: optical properties; nanostructured polymers; fibers

Received 3 October 2011; accepted 19 January 2013; published online
DOI: 10.1002/app.39147

INTRODUCTION

In the last few decades, organic/inorganic nanocomposites have attracted many attention in a variety of technological applications such as optical devices, biosensors, biomedical science, energy storage, and coating materials.[1,2] The manipulation of organic and inorganic phases greatly targets the properties of the resulting materials including composite nanofibers. They bring together the flexibility and light weight of organic materials and high strength, thermal, and chemical stability of inorganic materials.[3] The efficient performance reinforcing fillers should address proper orientation, efficient dispersion, narrow size distribution in nanoscale , interfacial interaction, and adequate surface compatibility with the matrix. These are extremely necessary to reach optimum properties regarding to specific mechanical, physical, and optical demands. Numerous techniques have been developed for preparation of composite fiber from micro to nanoscale. However, electrospinning is in top priority with regard to simplicity and extremely precise nanoscale process. Several studies have been reported to produce pure and composite of PVA nanofiber by electrospinning technique.[4–7] Hyun Woo and his coworkers used electrospinning technique to form the poly(vinyl alcohol) (PVA)/montmorillonite clay (MMT) nanofiber.[2] Another work focused on electrospun titanium dioxide/PVA nanocomposite fiber webs for application in multifunctional textiles.[2] The nanofiber scaffolds also were developed based on the electrospinning of poly(vinyl alcohol) (PVA)/gelatin aqueous solution.[2]

The TiO_2 is one of the most prominent multipurpose materials for variety of aspects such as gas sensors, dye-sensitized solar cells, photo catalysts, nonlinear optical devices, water purification, and self-cleaning.[4,5] Depending on the thermal and physical treatment, the TiO_2 shows several crystalline phases, such as rutile, brookite, and anatase. Among these three phases, the anatase can be used as photocatalyst and rutile is thoroughly used as white pigment in industry. The photoactivity for TiO_2 in anatase state can be potentially useful in solar energy conversion.[6] The latter specification highlights if TiO_2 organizes in large surface area. The electrospun nanofibers generally recognized as large surface area to volume ratio, small pore size, and high specific surface.[7] High specific surface makes opportunity for nanofibers to efficiently absorb the emitted light. This specification introduces nanofibers as a potential candidate for light absorption layer in solar cell device to convert solar energy to electrical energy. This vision opens new horizon to conduct investigation regarding to optical properties of nanofibers including photoactive materials. To best of our knowledge, no prior report on the optical properties of nanofibers composed of TiO_2 is available in the literature.

Several phenomena such as reflection, absorption, and scattering occurs once light passes through a material. The proportion of

each of them depends on numerous factors such as the refractive index, the size, and the shape of the separate phases and the physical properties of the matrix. The interaction of the light within the layer is described by absorbance and scattering coefficients. A number of theories such as Rayleigh scattering, Mie, Kubelka-Munk, and Geometric have been previously developed to study the optical properties of material.[8–10]

In general, the scattering behavior of particles depends on their size as ratio of particle size to wavelength. The ratio of fiber diameter to visible spectrum wavelength of 400–700 nm is more than one for conventional fiber in micrometer ranges. However, this ratio approach to a number less than one as electrospun fiber forms in nanoscale. In the same way, the optical properties of nanosized TiO_2 particle are different from conventional TiO_2 particle. Accordingly, the study of optical properties of nanosized particles is a novel and very interesting subjects. In this work, the bare PVA nanofibers and PVA nanofibers containing various amounts of TiO_2 nanoparticles were prepared using electrospinning technique. The effects of TiO_2 nanoparticle inclusion and the electrospun nanofiber geometry were investigated on optical properties of developed composite nanofiber substrate.

EXPERIMENTAL

Materials

Polyvinyl alcohol (PVA) with average molecular weight (M = 50,000–85,000) and degree of hydrolyzing $\geq$ 98% and titanium (IV) oxide (Anatase) nanoparticles with 10 nm diameter were purchased from Merck.

Instruments

The BANDELIN Sonicator (Sono Puls) was employed to disperse TiO_2 nanoparticles in PVA solution. Sartorius Professional meter PP-20 was used to measure the electrospinning solution conductivity. Scanning electron microscopy (SEM) (XL30, Netherland, Inc., Philips) and transmission electron microscopy (TEM) (CM120, Netherland, Inc., Philips) were used to analyze the diameters and morphologies of nanofibers. Reflective spectra was measured by a X-rite color Eye 7000A spectrophotometer between 400 nm to 700 nm wavelength with 10 nm interval and the accuracy of spectrometer was 0.01%. The CIELAB color parameter was measured under D65 illuminant and 10 degree standard colorimetric observer. The color and reflectance measurement was repeated four times for each sample. The average of color and reflectance was used. In the CIELAB system, the color parameters is expressed in terms of L^*(the lightness), a^* (the red-green value), b^*(the yellow-blue), C^*(chroma), and h (hue angle) values. The color difference between two samples is calculated by eq. (1).

$$\Delta E = \sqrt{(L_2^* - L_1^*)^2 + (a_2^* - a_1^*)^2 + (b_2^* - b_1^*)^2} \qquad (1)$$

where L_1^*, a_1^*, b_1^* are the color parameters of first sample, and L_2^*, a_2^*, b_2^* are the color parameters of second sample.

The electrospinning apparatus consist of a pump (Micro syringe Co. Ltd.) for dispensing of spinning solution through a syringe in a high voltage electric field. The DC power supply provide a range of voltage between 0 and 25 kV equipped with a positive and negative electrode respectively connects to syringe and collector.

Preparation of electrospinning solution

The electrospinning solution was composed of PVA and water with or without TiO_2 nanoparticles. PVA/TiO_2 nanocomposite solution was prepared by adding TiO_2 nanoparticles to PVA solution. In the first step, 0.01 g TiO_2 nanoparticles was sonicated for 30 minutes in 10 ml deionized water. Then, 0.8 g PVA was gradually added to the dispersed phase and sonicated for 30 minutes. Subsequently, a viscous solution produces for further processing. Ultrasonication generates alternating low-pressure and high-pressure waves in liquids, leading to the formation and violent collapse of small vacuum bubbles, and causes high-speed impinging liquid jets and strong hydrodynamic shear-forces. Hence, sonication brings the solution in higher temperature that needs to be cooled down using water bath.

Electrospinning of PVA/TiO_2 composite nanofibers

After the preparation of spinning solution, the solution was transferred to a 5 ml syringe and kept ready for spinning of nanofibers. The experiments were carried out on a horizontal electrospinning setup. The syringe containing PVA and PVA/TiO_2 solution was placed on a syringe pump (New Era NE-100)

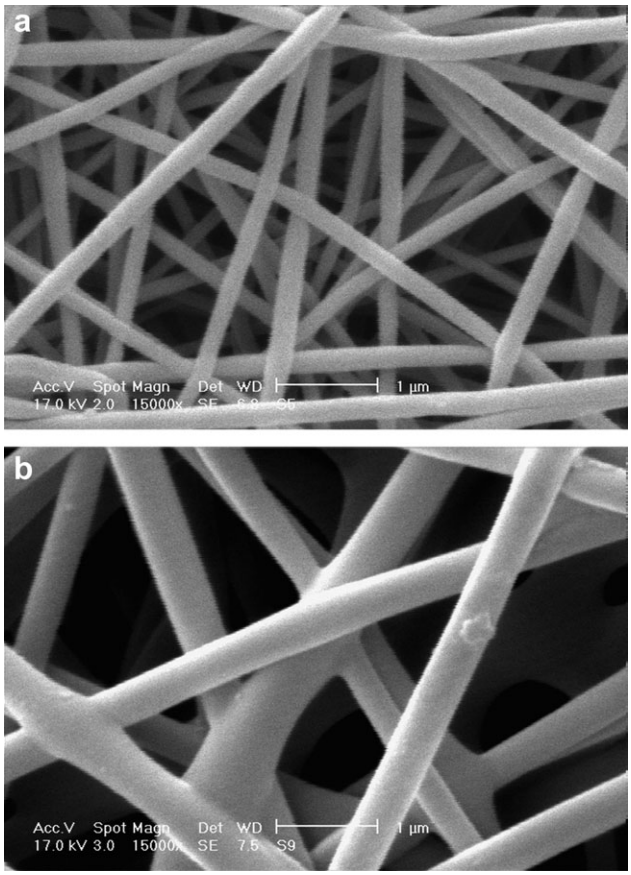

Figure 1. The SEM images of PVA nanofibers acquired using injection rate, tip to collector distance, and applied voltage, respectively, for samples (a) 10 cm, 19 kV, and 1 μl/min (b) 9 cm, 10 kV, and 5 μl/min.

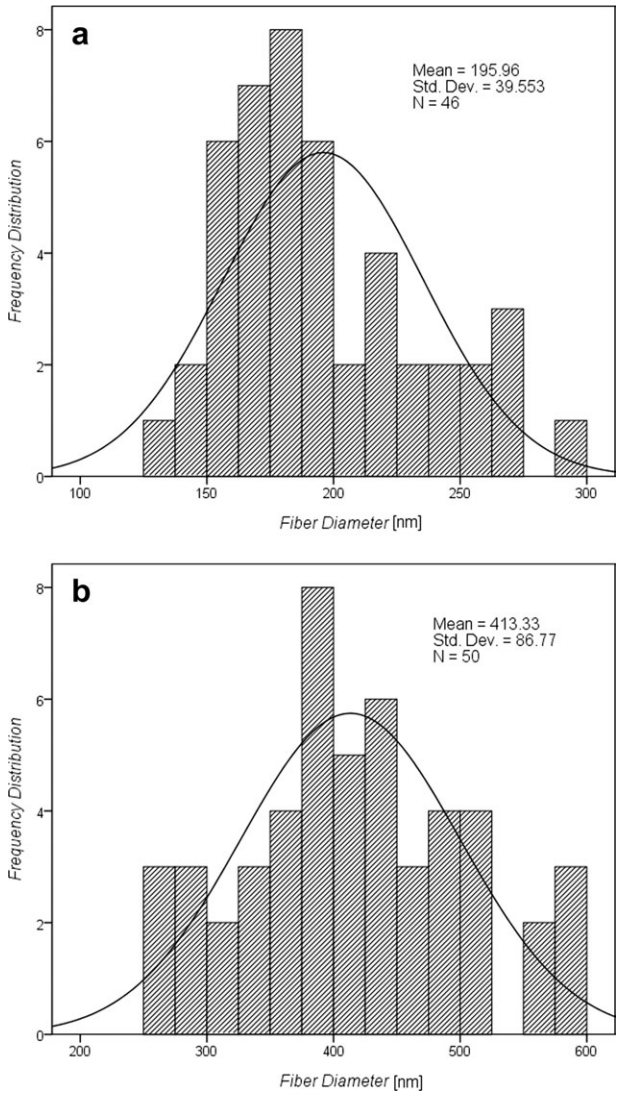

Figure 2. Frequency distribution of pure PVA nanofibers shown in (a) diameter = 195 ± 10nm based on Figure 1a (b) diameter = 413 ± 24 nm based on Figure 1b.

used to dispense the solution at a controlled rate. A high-voltage DC power supply (Gamma High Voltage ES-30) was used to generate the electric field needed for electrospinning. The positive electrode of the high-voltage supply was attached to the syringe needle via an alligator clip and the grounding electrode was connected to a flat collector wrapped with aluminum foil where electrospun nanofibers were accumulated to form a nonwoven mat. The electrospinning was carried out at room temperature. Subsequently, the aluminum foil was removed from the collector for further characterization.

RESULTS AND DISCUSSION

The change in optical properties in accordance to nanofiber geometry needs to be investigated through preparation of two distinct nanofiber samples with significant diameter difference. The electrospun nanofibers were collected by adjusting most effective operational parameters on nanofiber diameter including needle to collector distance, applied voltage, and injection rate. The operational parameters for producing first sample were adjusted on 10 cm, 19 kV, and 1 μl/min, respectively, for needle to collector distance, applied voltage, and injection rate. For the second sample, the needle to collector distance, the applied voltage, and the injection rate were 9 cm, 10 kV, and 5 μl/min, respectively. The SEM of samples 1 and 2 in same magnification are shown in Figure 1a and b, respectively. The nanofiber diameter measurement was carried out using technical analysis software to produce diameter frequency distribution graphs for both samples (Figure 2a and b).

Table I. Hiding power of pure PVA nanofibers in different diameters

	Diameter (nm)		
No.	Mean	Standard error	Hiding power
1	196	11	1.0009
2	413	24	0.9995

The average diameter and standard deviation of resulting PVA nanofibers for first sample was 195 ± 10 nm (Figures 1a and 2a). The reduction of distance and voltage to 9 cm and 10 kV, respectively, together with increase of injection rate to 5 μl/min

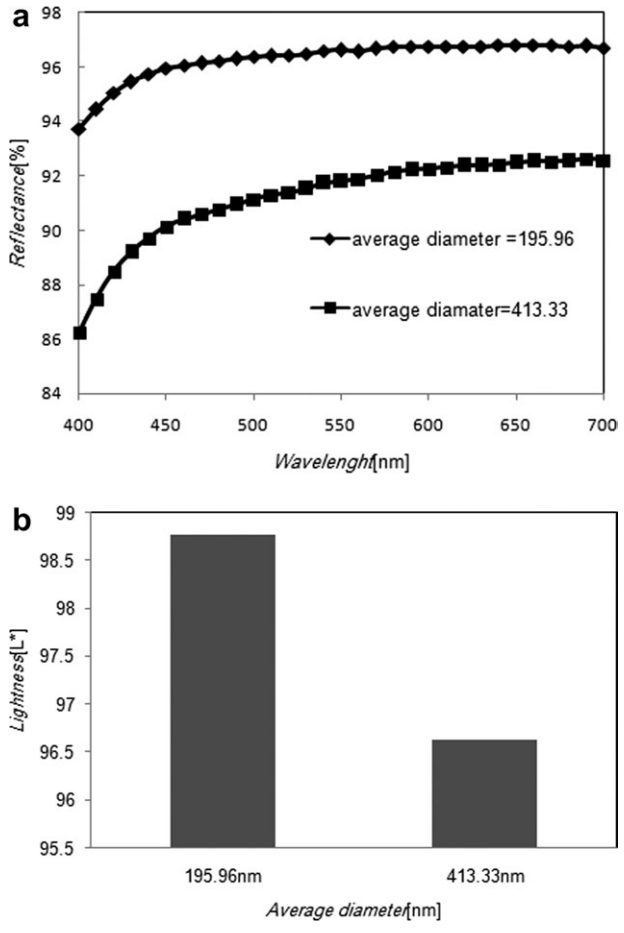

Figure 3. The reflectance spectra (a) and lightness (L^*) (b) of pure PVA nanofibers.

Table II. Comparison of illumination parameters of pure PVA nanofibers in different diameters

No.	Diameter (nm)	a*	b*	c*	h	RMS	ΔE
1	196	0.05	0.62	0.62	94.47	0.051	2.22
2	413	0.03	1.24	1.24	91.36		

leads to nanofibers with larger average diameter of 413 ± 24 nm (Figures 1b and 2b). The increase in nanofiber diameter as a function of cumulative effects of simultaneous decrease of distance and voltage in parallel to injection rate increase needs to be explained thoroughly.

The effect of spinning distance is not always the same. Spinning distance has a twofold effect on electrospun fiber diameter. Varying the distance has a direct influence on the jet flight time as well as electric field strength.

Longer spinning distance will provide more time for the jet to stretch in the electric field before it is deposited on the collector. Furthermore, solvents will have more time to evaporate. Hence, the fiber diameter will be prone to decrease. On the contrary, increasing the spinning distance will decrease the electric field strength ($E = V/d$), resulting in less acceleration, hence stretching of the jet, which leads to thicker fiber formation. The balance between these two effects will determine the final fiber diameter. Increase in fiber diameter[11–13] as well as decrease in fiber diameter[14] with increasing spinning distance was reported in the literature. There were also some cases in which spinning distance did not have a significant influence on fiber diameter.[15,16–18]

Applied voltage has two major different effects on fiber diameter. Firstly, increasing the applied voltage will increase the electric field strength and larger electrostatic stretching force causes the jet to accelerate more in the electric field, thereby favoring thinner fiber formation. Secondly, because charge transport is only carried out by the flow of polymer in the electrospinning process,[19] increasing the voltage would induce more surface charges on the jet. Subsequently, the mass flow rate from the needle tip to the collector will increase, say the solution will be drawn more quickly from the tip of the needle causing fiber diameter to increase. The combination of these two effects will determine the final fiber diameter. Hence, increasing applied voltage may decrease,[20–22] increase,[11,13,15] or may not change[15,23,24] the fiber diameter. Because of the given explanation, at low voltages, where the electric field strength is low, the effect of mass of solution could be dominant. Therefore, fiber diameter increases when the applied voltage rises. However, as the voltage exceeds a limit, the electric field will be high enough to be a determining factor. Hence, fiber diameter decreases as the voltage increases.

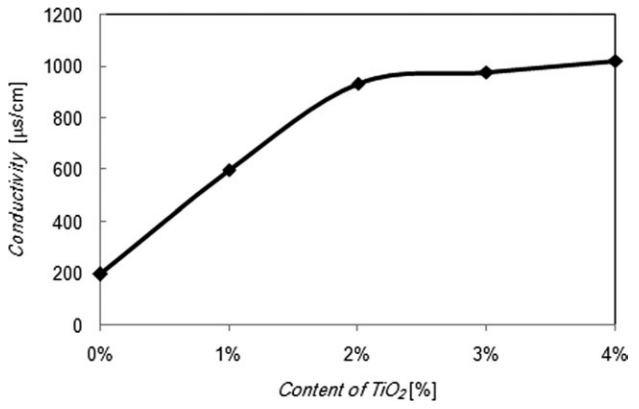

Figure 4. Conductivity of electrospinning solution versus increasing content of TiO_2.

It was suggested that a minimum value for solution flow rate is required to form the drop of polymer at the tip of the needle for the sake of maintaining a stable Taylor cone.[25] Hence, flow rate could affect the morphology of electrospun nanofibers such as fiber diameter. By increasing the flow rate, more amount of solution is delivered to the tip of the needle enabling the jet to carry the solution away faster. This could bring about an increase in the jet diameter, favoring thicker fiber formation.

The aforementioned finding clearly is in agreement with our observation when the dual effect of distance decreasing according to its impact on voltage increasing can be compensated by setting the voltage on lower value and a significant increase for injection rate. As a result, simultaneous decrease in distance and

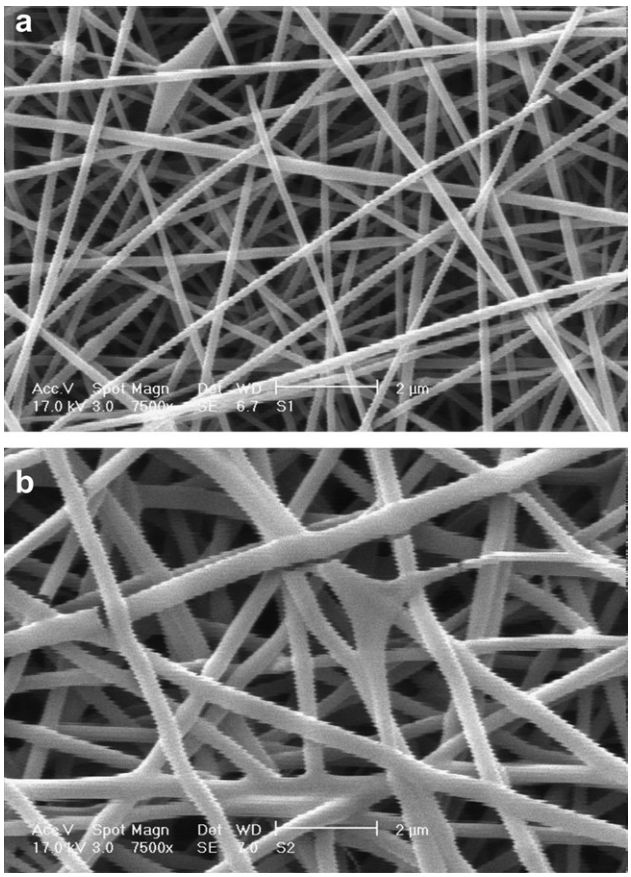

Figure 5. The SEM images of PVA nanofibers with 3% nano-TiO_2 acquired using injection rate, tip to collector distance, and voltage, respectively, for samples (a) 5 μl/min, 7 cm, and 11 kV (b) 5 μl/min, 7 cm, and 10 kV.

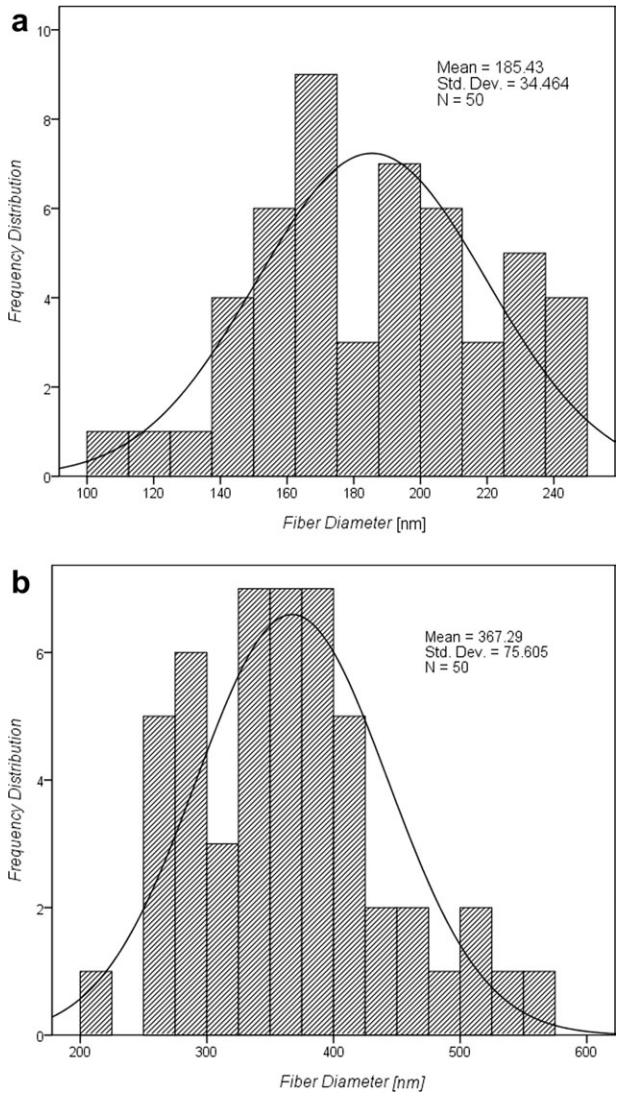

Figure 6. Frequency distribution of PVA/3% TiO_2nanofibers shown in (a) diameter = 185 ± 9 nm based on Figure 5a (b) diameter = 367 ± 20 nm based on Figure 5b.

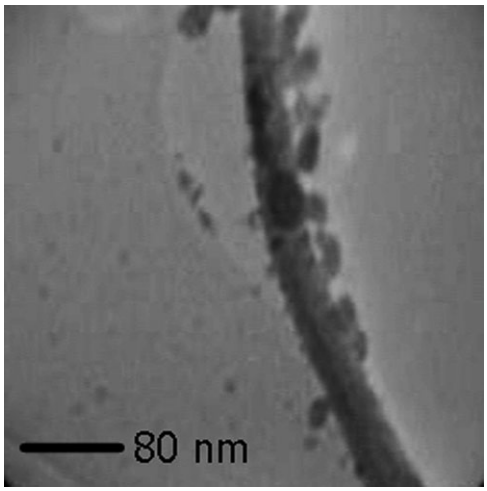

Figure 7. The TEM images of an individual PVA/ 3% TiO_2 nanofiber.

voltage plus injection rate increase guarantees the increase in nanofiber diameter and its distribution for further investigation.

The optical property of neat PVA nanofibers was investigated through reflectance spectra and colorimetric parameters of nanofibers using spectrophotometer. The reflectance spectra of the nanofibers were analyzed within the visible spectrum between 400 nm and 700 nm with 10 nm interval.

Initially, the optical opacity of samples was analyzed by measuring reflectance over white and black background. The opacity of samples was evaluated by calculating opacity factor or hiding power as eq. (2).

$$\text{opacity factor} = \frac{L^*_{\text{black}}}{L^*_{\text{white}}} \quad (2)$$

where L^*_{black} and L^*_{white} are the lightness of sample on the black and white background, respectively. The opacity factor of optically opaque sample is 1. The reflectance and optical properties of optically opaque sample do not depend on their thickness. The opacity factor or hiding power of PVA samples are shown in Table I. The measured opacity factor or hiding power value indicates that the all samples are opaque.

The reflectance spectra and lightness (L^*) of samples on gray background are shown in Figure 3a and b. As shown in these figures, the reflectance and lightness of sample with 195 ± 10 nm diameter is more than nanofibers with 413 ± 24 nm diameter. Nanofibers with smaller average diameter have larger specific surface area than nanofibers with larger average diameter so they have more reflectance and result to more lightness. The colorimetric parameters of samples are shown in Table II. As shown in this table, the color difference and reflectance spectra difference respectively are 2.22 ΔE^*_{ab} and 0.051 RMS.

The experimental setup was adjusted for spinning PVA/TiO_2 (3% w/w) by considering higher conductivity of nanocomposite solution. The TiO_2 nanoparticles change the conductivity of electrospinning solution. The relationship between conductivity and TiO_2 nanoparticle concentration is shown in Figure 4. The presence of well-dispersed TiO_2 can further increase the number of ions in the electrospinning solution. A further increase of ions can initiate the splitting up of subnanofibers from the main fibers.[26] So, the smaller voltage needs to produce nanofibers in the range of the bare PVA nanofibers. Hence, operational parameters consist of rate, distance, and voltage were kept respectively at 5 μl/min, 7 cm, and 11 kV. According to this condition, the diameter of produced PVA/TiO_2 nanofibers was

Table III. Hiding power of pure PVA/3% TiO_2 nanofibers in different diameters

	Diameter(nm)		
No.	Mean	Standard error	Hiding power
1	185	9	0.9995
2	367	21	0.993

Applied Polymer SCIENCE

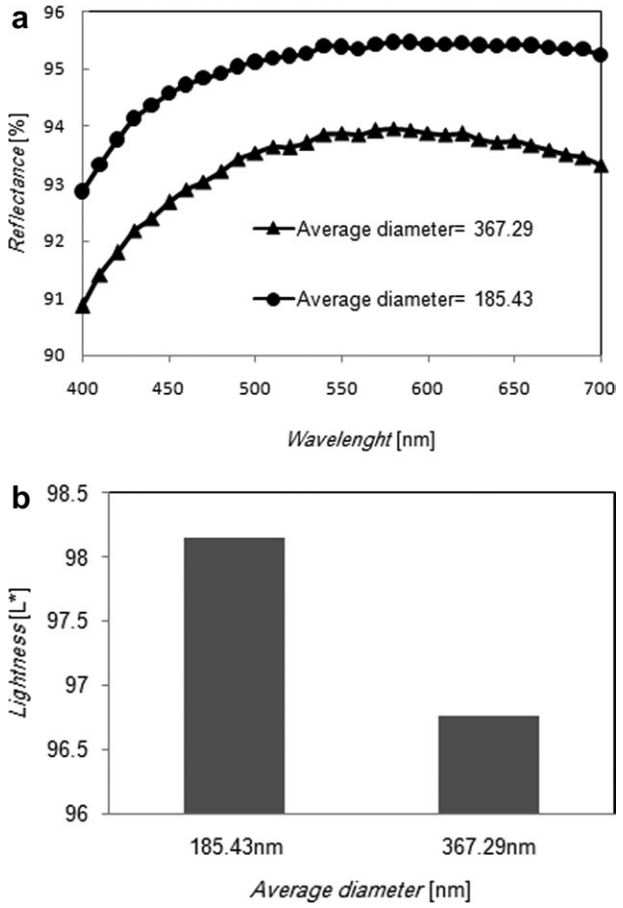

Figure 8. The reflectance spectra (a) and lightness (L^*) (b) of PVA/(3%) TiO_2 nanofibers.

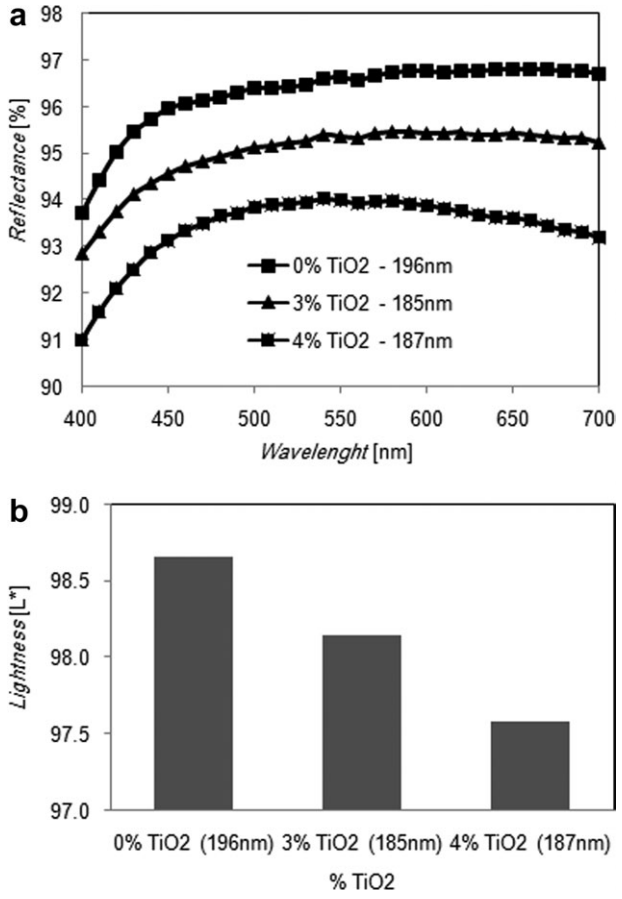

Figure 9. The reflectance spectra (a) and lightness (L^*) (b) of PVA with and without nano-TiO_2.

185 ± 9 nm (Figure 5a). To produce nanofibers with larger diameter, the voltage needs to be only reduced to 10 kV. In this condition, the diameter of nanofibers was 367 ± 20 nm (Figure 5b). The diameter frequency distributions of these nanofibers are shown in Figure 6a and b.

The TiO_2 nanoparticles change the nanofiber diameter, so that the diameter of PVA nanofiber containing TiO_2 nanoparticles is less than the pure PVA nanofiber in the same electrospinning condition. In general overview, the morphology of bare PVA nanofiber and its PVA/TiO_2 composite nanofiber counterpart is almost similar, which is essential to remove the effect of fiber diameter, porosity, and orientation on optical properties. However, some sort of roughness on fiber surface is evidenced as a consequence of TiO_2 nanoparticle. It can be distinguished based on the high magnification TEM picture, which highlights the nanofiber surface perturbation (Figure 7). Presumably, it develops distinct optical properties for PVA versus PVA/TiO_2 nanofiber.

Table IV. Colorimetric parameters of PVA/TiO_2 nanofibers in different diameters

No.	Diameter (nm)	a*	b*	c*	h	RMS	ΔE
1	185	−0.11	0.54	0.55	101.89	0.017	0.675
2	367	−0.03	0.53	0.53	93.51		

The opacity factor or hiding power of samples is shown in Table III. As shown in this table, the samples are opaque. The reflectance spectra and lightness (L^*) of samples on gray background are shown in Figure 8a and b. As shown in these figures, the reflectance and lightness of sample with 185 ± 9 nm diameter is more than nanofibers with 367 ± 20 nm diameter. The reflectance and lightness of sample decreased with increasing diameter of nanofibers. The colorimetric parameters of samples are shown in Table IV. As shown in this table, the color difference and reflectance spectra difference respectively are 0.675 ΔE^*_{ab} and 0.017 RMS.

The effect of TiO_2 nanoparticles on optical properties of PVA nanofibers are shown in Figure 9a and b for nanofibers with the same diameter. As shown in these figures, the reflectance of pure PVA nanofibers is more than PVA/TiO_2 composite nanofibers. Statistical test for matched pairs was used to comparing samples reflectance data of pure and 3% TiO_2 PVA/TiO_2 composite nanofibers. In statistic analyzing, the H_0: $DR = (R_2 - R_1) = 0$ is assumed in the null hypothesis. The 0.05 significant levels were used to test the claim that there is a difference between the reflectance spectra of PVA nanofiber with and without TiO_2 nanoparticles. The statistical test rejects the null hypothesis. There is sufficient evidence to

Table V. Colorimetric parameters of PVA nanofibers without and with nano-TiO_2

	Diameter (nm)								
No.	Mean	Standard error	% TiO_2	a*	b*	c*	h	RMS	ΔE
1	185	9	3	−0.11	0.54	0.55	101.89	0.013	0.628
2	196	11	0	0.05	0.62	0.62	94.47		
3	187	34	4	−0.3	0.56	0.64	117.97		

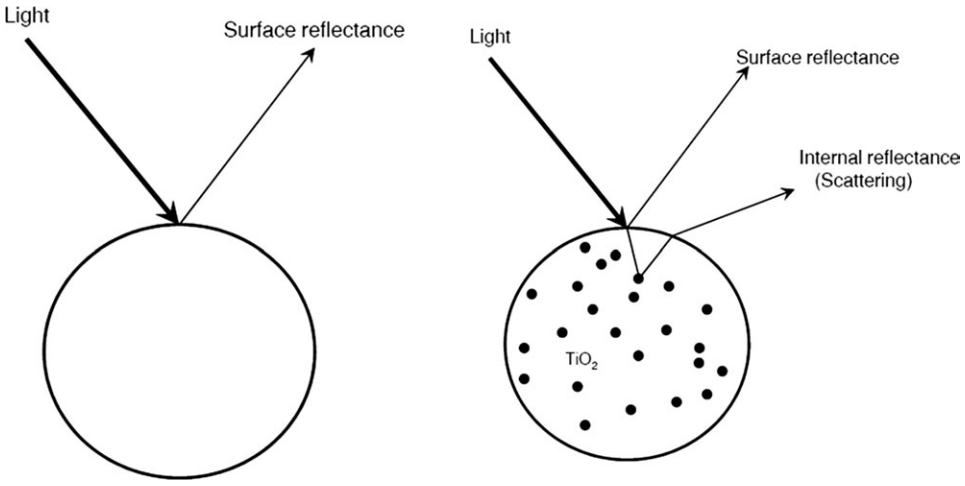

Figure 10. The light reflection of (a) PVA nanofibers without nano-TiO_2 (b) and with nano-TiO_2.

warrant rejection of the claim of no difference between the reflectance spectra of two samples. In addition, the colorimetric parameters of PVA nanofibers without and with 3% and 4% nano-TiO_2 are shown in Table V. As shown in this table, the color difference and reflectance spectra difference between pure and 3% TiO_2 PVA/TiO_2 composite nanofibers are 0.628 ΔE^*_{ab} and 0.013 RMS, respectively. The obtained results indicated that the effect of TiO_2 on a^*, b^*, and C^* are less than L^*. The a^*, b^*, and C^* variation is not significant. The color variation and color difference (ΔE) is because of lightness (L^*) variation.

When light is propagated through a fibrous matter, several physical phenomena such as interface surface reflection, absorption, and scattering occurs. The absorbance and scattering phenomena depends on the absorbance and scattering properties of polymer and particles in fibrous matter. But the surface reflectance depends on the refractive index and diameter of fibrous matter. So that the interface surface reflection increased with increasing refractive index. But, the interface surface reflectance decreased with increasing diameter. As shown in Figure 10, the reflectance of pure PVA nanofibers is because of interface surface reflectance. However, the reflectance of PVA nanofibers containing TiO_2 nanoparticle is because of interface surface reflectance and internal reflectance as scattering properties of TiO_2 nanoparticle.

CONCLUSION

This work explained the effects of TiO_2 nanoparticle and nanofiber diameter on optical properties of PVA nanofibers. Initially, the neat PVA nanofibers and PVA nanofibers containing titanium dioxide nanoparticles were prepared by electrospinning technique in two ranges of diameters. Subsequently, the effect of TiO_2 nanoparticle and nanofiber diameter on its optical properties as reflectivity of light and color was studied. The obtained results indicated that the reflectance and lightness of nanofibers decreased with increasing diameter. Also, the reflectance and lightness of nanofibers decreased with adding nano-TiO_2 particles. The reflectance of pure PVA nanofibers was due to interface surface reflectance. But, the reflectance of PVA nanofibers with TiO_2 was because of interface surface reflectance and internal reflectance or scattering of TiO_2 nanoparticles. This delustered nano layer can be use in clothing and micro optical electronic device as a very fine fibrous opaque material. Also, it can be used as an antibacterial and UV-protective nanoweb.

REFERENCES

1. Mahendia, S.; Chahal, R. P.; Goyal, P.; Kumar, S. Optical and structural properties of poly(vinyl alcohol) films embedded with citrate-stabilized gold nanoparticles. *J. Phys. D: Appl. Phys.*, **2011**, *44*, 1.

2. Andrady, A. L. Science and Technology of Polymer Nanofibers. **2008**, John Wiley & Sons, Inc.: Hoboken, New Jersey.

3. Wu, H.; Fan, J.; Qin, X.; Zhang, G. Characterization of PVAc/TiO2 Hybrid Nanofibers: From Fibrous Morphologies to Molecular Structures. *Appl. Polym. Sci.* **2009**, *112*, 1481.

4. Cheuk, K.; Wei-ning, Z.; Chen, W.; Chang-fa, X. Low temperature preparation of nano TiO2 and its application as antibacterial agents. *Trans. Nonferrous Met. Soc. China*, **2007**, *17*, 700.
5. Park, J. A.; Moon, J.; Lee, S. J.; Kim, S. H.; Zyung, T.; Chu, H. Y. Structural, electrical and gas sensing properties of eletrospun TiO2 nano fi bers. *Thin Solid Films*, **2010**, *518*, 6642.
6. Khanna, P. K.; Singh, N.; Charan, S. Synthesis of nano-particles of anatase-TiO2 and preparation of its optically transparent film in PVA. *Mater. Lett.*, **2007**, *61*, 4725.
7. Nien, Y. H.; Lin, P. J.; Wu, L. Y.; Liou, T. H.; Wey, P. I. Preparation of Poly(vinyl alcohol)/TiO2 Nanofibers by Electrospinning ww.nt.ntnu.no/users/skoge/prost/proceedings/aiche-2004/pdffiles/papers/577f.pdf.
8. McDonald, R. Colour Physics for Industry. **1997**, Society of Dyers and Colourists.
9. Chaudhury, A. K. R., Modern Concepts of Color and Appearance **2000**, Science Publishers, Inc: USA.
10. Volz, H. G. Industrial Color Testing: Fundamental and Technique, 2nd Ed.; Wiely-VCH: New York, **2001**.
11. Li, Q.; Jia, Z.; Yang, Y.; Wang, L.; Guan, Z. Preparation and properties of poly(vinyl alcohol) nanofibers by electrospinning, Proceedings of IEEE International Conference on Solid Dielectrics, Winchester, U.K. (**2007**).
12. Jarusuwannapoom, T.; Hongrojjanawiwat, W.; Jitjaicham, S.; Wannatong, L.; Nithitanakul, M.; Pattamaprom, C.; Koombhongse, P.; Rangkupan R.; Supaphol, P. *Eur. Polym. J.*, **2005**, *41*, 409.
13. Baker, S. C.; Atkin, N.; Gunning, P. A.; Granville, N.; Wilson, K.; Wilson D.; Southgate, J. *Biomaterials*, **2006**, *27*, 3136.
14. Wang T.; Kumar, S. *J. Appl. Polym. Sci.*, **2006**, *102*, 1023.
15. Zhang, C.; Yuan, X.; Wu, L.; Han Y.; Sheng, J. *Eur. Polym. J.*, **2005**, *41*, 423.
16. Sukigara, S.; Gandhi, M.; Ayutsede, J.; Micklus, M.; Ko, F. *Polymer*, **2003**, *44*, 5721.
17. Yuan, X.; Zhang, Y.; Dong, C.; Sheng, J. *Polym. Int.*, **2004**, *53*, 1704.
18. Ki, C. S.; Baek, D. H.; Gang, K. D.; Lee, K. H.; Um, I. C.; Park, Y. H. *Polymer*, **2005**, *46*, 5094.
19. Deitzel, J. M.; Kleinmeyer, J.; Harris, D.; Beck Tan, N.C. *Polymer*, **2001**, *42*, 261.
20. Buchko, C. J.; Chen, L. C.; Shen, Y.; Martin, D. C. *Polymer*, **1999**, *40*, 7397.
21. Lee, J. S.; Choi, K. H.; Ghim, H. D.; Kim, S. S.; Chun, D. H.; Kim H. Y.; Lyoo, W. S. *J. Appl. Polym. Sci.*, **2004**, *93*, 1638.
22. Fennessey S. F.; Farris R. J. *Polymer*, **2004**, *45*, 4217.
23. Tan, S.-H.; Inai, R.; Kotaki, M.; Ramakrishna, R. *Polymer*, **2005**, *46*, 6128.
24. Kidoaki, S.; Kwon, I. K.; Matsuda, T. *Biomaterials*, **2005**, *26*, 37.
25. Zong, X.; Kim, K.; Fang, D.; Ran, S.; Hsiao, B. S.; Chu, B. *Polymer*, **2002**, *43*, 4403.
26. Pant, H. R.; Bajgai, M. P.; Nam, K. T.; Seo, Y. A.; Pandeya, D. R.; Hong, S. T.; Kim, H. Y. *J. Hazard. Mater.*, **2011**, *185*, 124.